20th Australasian Fluid Mechanics Conference
Perth, Australia
5-8 December 2016

Low Speed Aerodynamics and Static Stability of Hypersonic Vehicles

T. Bykerk[1], D. Verstraete[1], G.A. Vio[1] and J. Jeyaratnam[1]

[1]School of Aerospace, Mechanical and Mechatronic Engineering, The University of Sydney, New South Wales 2006, Australia

Abstract

Hypersonic vehicle design usually focuses on the aerodynamic, structural and thermal challenges at high Mach numbers. The stability and handling qualities at low speeds are often not considered, however, when the design is intended to transport passengers, they are crucial.

In this paper the low speed aerodynamics and static stability characteristics of two different hypersonic vehicles are analysed numerically using CFD and experimentally through low speed wind tunnel testing. The focus of the CFD studies is to determine subsonic flow features as well as aerodynamic and static stability derivatives. The experimental testing uses a number of flow visualisation methods to validate the flow features found in the CFD studies.

Results indicate that there may be issues with vortices originating from the nose of both aircraft at high angles of attack, which make contact with the leading edges of the fins. Some potential stability issues are also identified at angles of attack which would be typical at landing and take-off.

Introduction

Interest in developing vehicles which can drastically reduce travel time between major world cities is on the increase. Air breathing aircraft capable of travelling in excess of five times the speed of sound, also known as hypersonic waveriders, are a possible solution. Their ability to travel at speeds in excess of Mach 5 would mean a cutting down the travel time between Australia and Europe significantly.

Research into hypersonic aircraft is mainly confined to analysis of the technology required for the design operating point [6]. Despite the need for these vehicles to operate at subsonic speeds during landing and take-off phases, research into the low speed segments of these flights is limited. This is potentially problematic as a high speed optimised vehicle can become unstable at low speed or would require excessive angle of attack (*AoA*) and speed to land. The latter would have major effects on pilot visibility and long runway lengths.

Major differences in geometry exist between an optimum hypersonic vehicle (sharp and angular) and a subsonic aircraft (blunt and rounded). The high speed design features have a negative effect on the low speed performance of the vehicle, as sharp geometry induces flow separation, generally resulting in high drag and low lift. To have the most viable aircraft, a compromise must be sought to increase the subsonic performance while not severely impacting the hypersonic aerodynamics, stability or efficiency.

During the late 1990's NASA contracted Accurate Automation Corporation (AAC) to undertake the LoFLYTE™ program, where the low speed flight regime of an optimised Mach 5.5 waverider was investigated [4]. Overall conclusions were that the low speed characteristics of LoFLYTE™ were satisfactory and speeds for take-off and landing were achievable. Using laser light sheet flow visualisation, strong leading edge vortices were observed and improved the lift characteristics. Tests conducted with both tail on and tail off showed that vortex/fin interactions reduced the gradient of the lift curve. The aircraft also had a minor pitch up tendency, which increased in severity with *AoA*.

A pitch up tendency is typical among delta-winged aircraft, with similar behaviour shown by Concorde [9]. While leading edge flow separation and subsequent vortex formation improve lift, vortex breakdown with increasing *AoA* has been shown to result in a non-linear, destabilising pitching moment [1, 11].

Low speed investigations were also performed as part of the X-43A program, which successfully undertook Scramjet powered flight up to Mach 9.68 [7]. A low speed variant was tested by AAC [2]. The X-43A-LS was an unmanned aerial vehicle, remotely piloted from the ground. The aircraft varied slightly from the high speed vehicle, with the wings and fins being enlarged, as well as the centre of gravity shifted [3]. The investigation concluded that the aircraft was stable both longitudinally and laterally [2,3]. This showed that for a completely viable vehicle, a compromise between the differing geometries of the high and low speed versions is needed.

The Japanese Aerospace Exploration Agency (JAXA) has experimented with changing geometry of their hypersonic vehicle to increase the low speed performance. Taguchi et. al. examine their vehicle at Mach 0.3 and at 10 degrees *AoA* both computationally and experimentally [10]. CFD simulations show that two large vortices form as a result of the flow rolling up from the underside of the vehicle over the top surface similar to those shown in ref. [4].

In this paper the Michigan AFRL cruiser and the Hexafly-Int vehicle are presented and examined through a range of *AoA* and angles of sideslip (*AoS*).

Methodology

A numerical analysis using the CFD solver ANSYS Fluent was performed on both vehicles to estimate aerodynamic and stability coefficients. Longitudinal studies were conducted using a half vehicle mesh with a symmetry plane. Lateral studies required a full vehicle mesh. The realisable k-ε turbulence model was used at a Reynolds number of approximately 1.5×10^6. This Reynolds number was chosen to match the conditions in the 3x4 ft wind tunnel tests. Additional tests were conducted in a smoke tunnel at a Reynolds number of 1.75×10^5.

An unstructured tetrahedral mesh was created with 15 prism inflation layers around the vehicle. The far field extended approximately 10 chord lengths upstream and 15 chords downstream. As shown in Figure 1, the far field is a C-style grid with two bodies of influence to refine the mesh as it approaches the vehicle. Longitudinal studies were completed for an *AoA* range of -5 to 15 degrees. Lateral studies were completed for an *AoS* range of -10 to 10 degrees. The sideslip angles were also run through a range of *AoA* up to 8 degrees for the Hexafly-Int vehicle and 4 degrees for the Michigan AFRL cruiser.

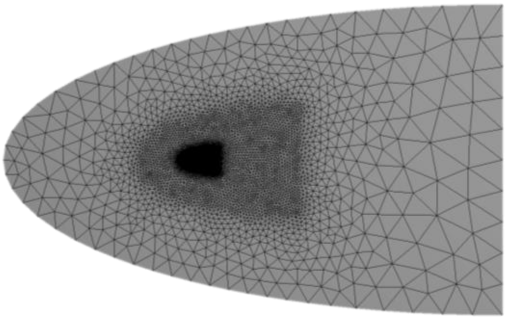

Figure 1. Half body mesh typical of the Michigan AFRL cruiser and Hexafly-Int vehicles containing approximately 15x10^{6} elements.

The physical characteristics the scaled vehicle are presented in Table 1.

Characteristic	Hexafly-Int	AFRL Cruiser
Reference Area	0.122 m^2	0.146 m^2
Reference Chord Length	0.723 m	0.762 m
Reference Full Span	0.273 m	0.284 m

Table 1. Physical characteristics of scaled vehicles.

The locations of the *CoG* are marked in Figure 2. For the Hexafly-Int vehicle, the *CoG* location was scaled from ref. [8].

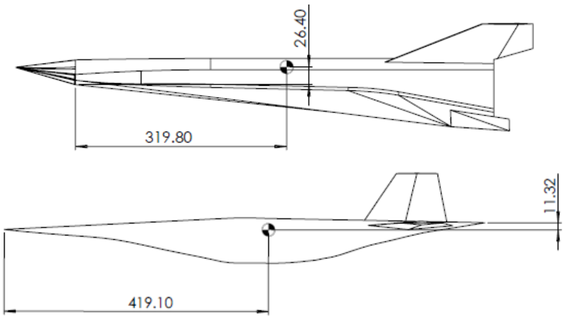

Figure 2. *CoG* location for Hexafly-Int (top) and AFRL Cruiser (bottom)

A model of the Michigan AFRL cruiser was fabricated using a laser cut wooden frame filled with high density foam and fibre glassed. White tufts were attached to the top surface of the vehicle to contrast with the black painted model. The experimental setup in the 3x4 ft wind tunnel is shown in Figure 4.

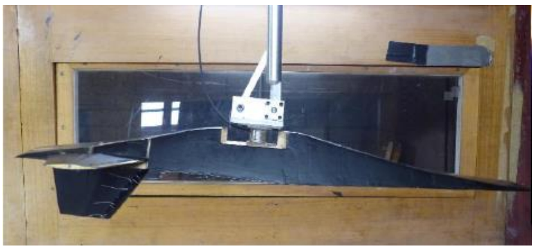

Figure 3. Experimental setup of 3x4 ft Michigan AFRL cruiser wind tunnel model.

A 250mm long SLS 3D printed model of each vehicle was additionally tested in the University of Sydney low speed smoke tunnel. The experimental setup in the smoke tunnel is shown in Figure 4.

Figure 4. Experimental setup of Hexafly smoke tunnel model.

Results and Discussion

Results for the Hexafly-Int vehicle are compared with earlier research of this vehicle using TRANAIR, a 3D potential flow solver. These are for comparison only and are found in ref. [5].

Hexafly-Int

Figure 5 presents results for C_L vs *AoA*. Increasing the *AoA*, leading edge vortices appeared and continued to increase in strength up to 15 degrees as in ref. [4]. The CFD results show a Mach 0.25 landing speed at 8 degrees *AoA* is achievable.

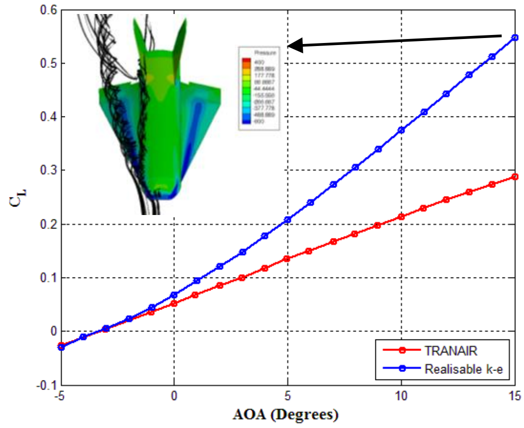

Figure 5. CFD and TRANAIR results of Hexafly C_L vs *AoA* showing strong leading edge vortices for the 15 degree *AoA* case.

Figure 6 presents results for C_m vs *AoA*. The CFD results indicate stability up to 10 degrees *AoA* ($C_{m\alpha} < 0$), with a transition to instability as *AoA* is increased further. This pitch up tendency is consistent with similar aircraft [1, 4, 9] and is attributed to a shifting centre of pressure due to leading edge vortex behaviour as discussed in ref. [1].

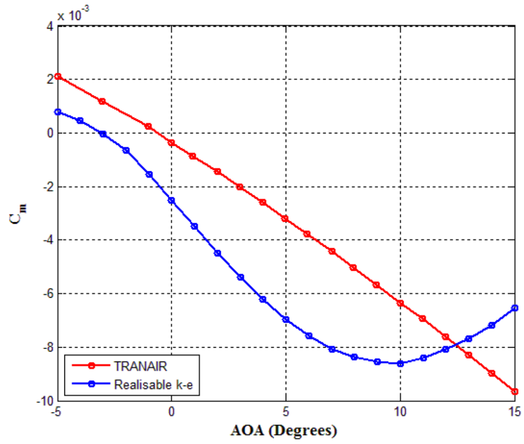

Figure 6. CFD and TRANAIR results of Hexafly C_m vs *AoA*.

Figure 7 shows that at low *AoA* the vehicle is unstable in roll ($C_{l\beta}$ > 0). This can be attributed to its low mounted wing with anhedral [5]. The wing configuration of this aircraft is a fundamental requirement of the Mach 7.4 design point, highlighting the potential susceptibility of these types of vehicles to roll instability.

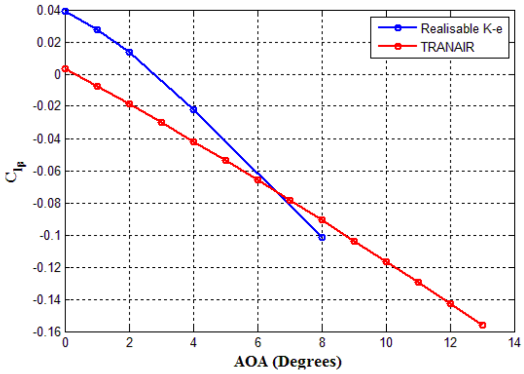

Figure 7. CFD and TRANAIR results of Hexafly roll moment coefficient gradient for increasing *AoA*.

The CFD results show the inherent non-linear nature of slender delta wings at low speed. The contrasting linear results obtained from TRANAIR show the limitations of using potential flow solvers for these types of aircraft. The significant under prediction of lift, as well as over prediction in pitch stability is expected when considering the results found in refs. [1, 4, 9]. The difference between results for the lateral stability cases is attributed to the asymmetric vortex formation at *AoS* which can be seen in

Figure 9.

The remaining static stability derivatives from the CFD studies show a stable vehicle are presented in Table 2.

Derivative	Minimum Calculated	Maximum Calculated
$C_{Y\beta}$	-0.65	-0.64
$C_{n\beta}$	0.354	0.43

Table 2. Summary of side force and yaw static stability derivatives.

Images of the CFD results and smoke tunnel test for 15 degrees *AoA* are compared in Figure 8. The location of the leading edge vortices in the smoke tunnel are consistent with the CFD results while the vortices interacting with the fins appear to be slightly higher in the smoke tunnel. The core of this vortex is also seen to be larger than the leading edge vortices in both CFD and experimental results, indicating relative weakness.

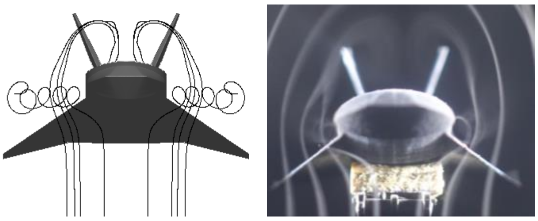

Figure 8. Comparison of vortex behaviour for Hexafly-Int Vehicle seen in CFD (left) and smoke tunnel (right) at 15 degrees *AoA*.

Figure 9 shows an agreement in terms of the asymmetric vortex formation at high *AoS*. The exact location of the vortex differs as the smoke tunnel model was subjected to a much higher angle of sideslip than was tested in CFD.

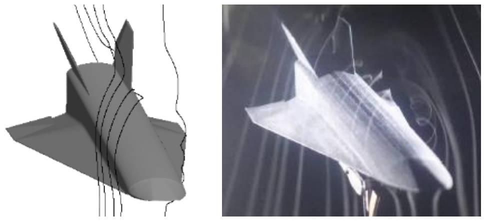

Figure 9. Asymmetric vortex in CFD (left) and smoke tunnel (right).

Michigan AFRL Cruiser

Table 3 shows a summary of the aerodynamic and stability derivatives from the CFD studies. The vehicle is stable, but has very poor lifting characteristics. This can be attributed to the lack of wing area.

Derivative	Minimum Calculated	Maximum Calculated
$C_{L\alpha}$	0.881	
C_{L0}	-0.0231	
$C_{m\alpha}$	-0.354	
C_{m0}	0.0151	
$C_{Y\beta}$	-0.335	-0.285
$C_{l\beta}$	-0.055	-0.0275
$C_{n\beta}$	0.048	0.085

Table 3. Michigan AFRL cruiser aerodynamic and stability derivatives.

Figure 10 presents the top surface contours and streamlines for increasing *AoA*. In these images, vortices from the nose begin to appear at 5 degrees *AoA*. The vortices increase in strength up to 15 degrees. These vortices continue downstream where they impinge on the leading edge of the fin. At 15 degrees *AoA* significant separation occurs at the nose of the body due to the adverse pressure gradient (Figure 10 (d)).

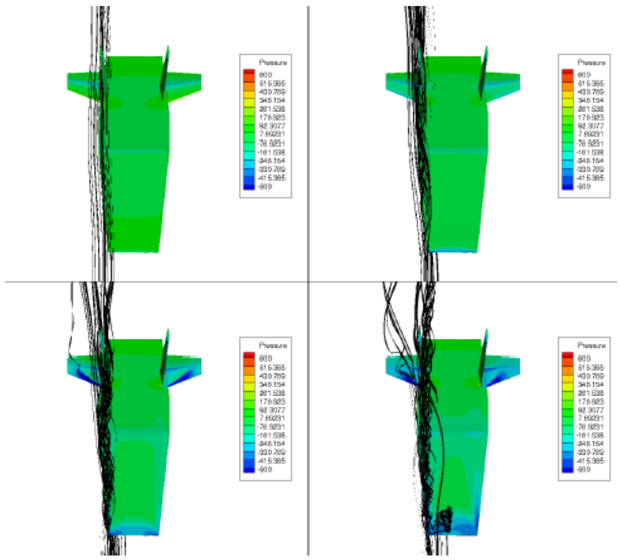

Figure 10. Michigan AFRL Cruiser vortex formation at (a) 0 degrees *AoA* (top left), (b) 5 degrees *AoA* (top right), (c) 10 degrees *AoA* (bottom left) and (d) 15 degrees *AoA* (bottom right).

Figure 11 shows the vortex at ten degrees *AoA*. The location of this vortex is similar to the vortex presented by JAXA in ref. [10].

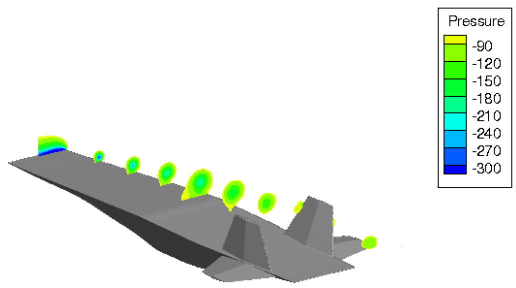

Figure 11. Vortex formation and fin interaction of Michigan AFRL cruiser (right) at 10 degrees *AoA*.

Qualitative features of the CFD results were validated in the 3x4 ft wind tunnel using tuft flow visualisation. Figure 12 shows the effect of the growing vortex on the fin tufts with increasing angle of attack.

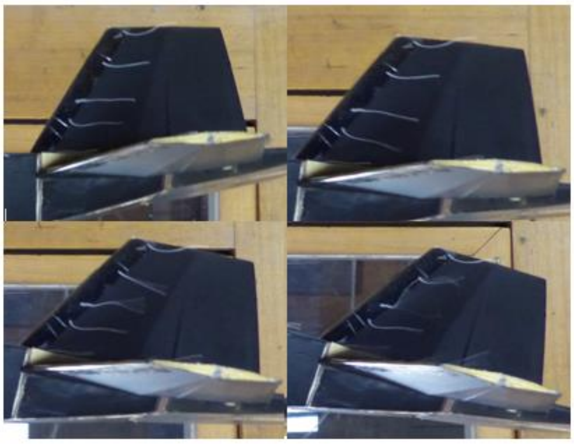

Figure 12. Tuft flow visualisation of the Michigan AFRL Cruiser vortex/fin interaction at (a) 0 degrees *AoA* (top left), (b) 5 degrees *AoA* (top right), (c) 10 degrees *AoA* (bottom left) and (d) 15 degrees *AoA* (bottom right).

Further validation of the flow was seen in the smoke tunnel. Figure 13 shows a comparison between CFD and smoke tunnel flow visualisation. Both the location and size of the vortices interacting with the fins are in agreement.

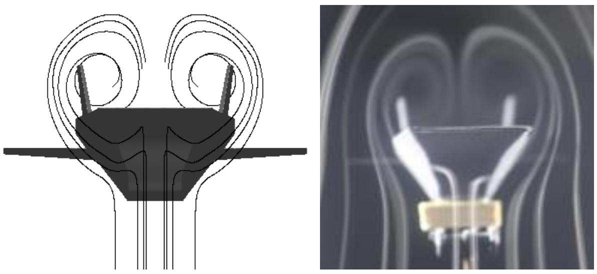

Figure 13. Comparison of vortex behaviour for Michigan AFRL cruiser seen in CFD (left) and smoke tunnel (right) at 15 degrees *AoA*.

Conclusion

Hypersonic waveriders and most of their required technology have been successfully demonstrated over the past 15 years and the movement towards making hypersonic travel a reality is well underway. Often the low speed spectrum of hypersonic flight is neglected, leaving a gap in the understanding of the bigger picture – how these vehicles will become commercially viable with stable low speed landings and take-offs.

In this paper the low speed aerodynamics and static stability of two hypersonic vehicles is investigated. From these investigations the following conclusions can be drawn:

- CFD results show that the Hexafly-Int delta wing waverider has superior low speed lift qualities compared to the Michigan AFRL Cruiser.
- A landing speed for the Hexafly-Int vehicle of Mach 0.25 is achievable with an angle of attack of approximately 8 degrees.
- The delta wing planform of Hexafly showed stability issues in pitch above 10 degrees angle of attack, due to a shifting centre of pressure caused by vortex lift.
- The anhedral delta of the Hexafly-Int vehicle results in low speed roll instability below 2.7 degrees angle of attack.
- The Michigan AFRL Cruiser is stable for all flight conditions with a centre of gravity location of 55% of the fuselage length.
- CFD showed vortices originating from the nose at high angles of attack and interacting with the fins of both vehicles as well as asymmetric vortices at high angles of sideslip. Smoke tunnel tests validated these results.
- The testing conducted in the 3x4 ft wind Tunnel validated the existence of vortices interacting with rear fins on Michigan AFRL Cruiser.

This project has created the groundwork for further research into the two vehicles presented. There is significant scope for future work, including numerical and experimental analysis.

Acknowledgments

This work was performed within the 'High Speed Experimental Fly Vehicles - International' (HEXAFLY-INT) project fostering International Cooperation on Civil High-Speed Air Transport Research. HEXAFLY-INT, coordinated by ESA-ESTEC, is supported by the EU within the 7th Framework Program Theme 7 Transport, Contract no.: ACP3-GA-2014-620327. The project is also supported by the Ministry of Industry and Trade, Russian Federation. Further information on HEXAFLY-INT can be found on http://www.esa.int/techresources/hexafly_int.

The authors would like to thank Prof. Carlos Cesnik of Michigan University for providing the geometry of the AFRL cruiser.

References

[1] Benoleil, A. (1994). Aerodynamic pitch-up of cranked arrow wings estimation, trim, and configuration design. Virginia: Virginia Polytechnic Institute & State University.

[2] Gibson, C., Neidhoefer, J., Cooper, S., Carlton, L. & Cox, C. (2002). Development and flight test of the X-43A-LS hypersonic configuration UAV. AIAA's 1st Technical Conference and Workshop on Unmanned Aerospace Vehicles.

[3] Gibson, C., Vess, R. & Pegg, R. (2003). Low speed flight testing of a X-43A hypersonic lifting body configuration. 12th AIAA International Space Planes and Hypersonic Systems and Technologies.

[4] Hahne, D (1997). Evaluation of the Low-Speed Stability and Control Characteristics of a Mach 5.5 Waverider Concept. Virginia: NASA.

[5] Jeyaratnam, J.J. & Verstraete, D., Analysis of low speed stability derivatives of a hypersonic test vehicle, APISAT 2015 - 7th Asia-Pacific International Symposium on Aerospace Technology, pp.266-275, 2015

[6] Küchemann, D. (1965). Hypersonic Aircraft and Their Aerodynamic Problems. Progress in Aerospace Sciences. 6 (1), pp.271-353.

[7] McClinton, C. (2006). X-43 - Scramjet Power Breaks the Hypersonic Barrier. 44th AIAA Aerospace Sciences Meeting and Exhibit.

[8] Pezella, G., Marini, M., Reimann, B & Steelant, J. (2015). Aerodynamic Design Analysis of the Hexafly-Int Hypersonic Glider. 20th AIAA International Space Planes and Hypersonic Systems and Technologies Conference.

[9] Rech, J. & Leyman, C (1980). A Case Study by Aerospatiale and British Aerospace on the Concorde. USA: AIAA.

[10] Taguchi, H., Kobayashi H., Takayuki, K., Ueno, A., Imamura, S., Hongoh, M. & Harada, K. (2012). Research on Hypersonic Aircraft using Pre-Cooled Turbojet Engine. Acta Astronautica. 73 (1), pp.164-172.

[11] Verhaagen N. G. and Maseland J. E. J. Investigation of the vortex flow over a 76/60° double delta wing at 20 ° incidence. AIAA-91-3208-CP, pp.70-80, 1991.